PROCEEDINGS OF SPIE

SPIEDigitalLibrary.org/conference-proceedings-of-spie

Advancement of an optical remote sensing model to simulate the underwater light field

Charles R. Bostater
Wei-ming Ma
Ted McNally

SPIE.

Advancement of an optical remote sensing model to simulate the underwater light field

Charles Bostater, Wei-ming Ma, and Ted McNally

Marine and Environmental Optics Laboratory, Center for Remote Sensing
Marine and Environmental Systems Division
Florida Institute of Technology
150 West University Blvd.
Melbourne, FL 32937

ABSTRACT

An analytical solution to the two-flow equations developed by Bostater, et al.[1] is modified, and a sensitivity analysis is performed on the remote sensing model which contains both diffuse and specular light components. The resulting model simulates the solution to two different cases of the two-flow equations. The Case I model uses the two-flow irradiance equations where sub-surface collimated or specular irradiance is evaluated implicitly. All of the irradiance is assumed to become completely diffuse when it enters the water column. The Case II model uses equations that explicitly include collimated irradiance in the water column. Both models are simulated in three different ways in this paper based on the vertical distribution of the constituents in the water column. The concentrations of the water quality parameters can be assumed (a) constant with depth, (b) divided into three distinct layers with different concentrations in each layer, or (c) divided into n layers of differing concentrations. The solutions to the two-flow equations with (Case II) and without (Case I) the specular, collimated irradiance and assuming a uniform water column, are given by Bostater et. al.[2]. This paper focuses on the derivation of the layered Case I and II models, a sensitivity analysis performed on the Case II model coefficients, and comparisons of the output from the differing model assumptions are presented.

1. INTRODUCTION

The transfer of the sun's radiant energy through natural waters has been studied by numerous authors[4,5,6]. These authors, and others, have realized the usefulness of quantitative models to describe the physical processes of radiative transfer in natural waters for predicting the light field in water. At the base of most of these equations, or models, is radiative transfer theory. If one ignores sources of radiant energy and inelastic scattering within the hydrological medium, then all energy impinging on a unit volume of a medium is either absorbed, scattered, or transmitted through the medium. Any model that one hopes to use to describe the underwater light field needs to consider the these processes.

Priesendorfer[6] gives a version of the radiative transfer equation (RTE) as:

$$\mu \frac{dL(z;\xi;\lambda)}{dz} = -c(z;\lambda)L(z;\xi;\lambda) + \int_{\Xi} L(z;\xi';\lambda)\beta(z;\xi' \rightarrow \xi;\lambda)d\Omega(\xi') + \beta(z;\xi' \rightarrow \xi;\lambda)L_c(z;\xi) \quad (1)$$

where $\mu=\cos\theta$ (cosine of the zenith angle), L is radiance ($Wm^{-2}sr^{-1}$), z is depth (m) positive downward, ξ is the direction of the light, λ is the wavelength (nm), c is the beam attenuation coefficient (absorption + scattering) (m^{-1}), Ξ indicates integration over all directions in the unit sphere, β is the volume scattering function ($m^{-1}sr^{-1}$) that indicates the amount of light originally heading in direction ξ' at depth z elastically scattered into direction ξ (by elastic scattering we mean scattering with no change in wavelength, whereas inelastic scattering is scattering that involves a change of wavelength), and L_c is the collimated radiance ($Wm^{-2}sr^{-1}$). The first term on the right hand side of 1 is the loss of radiant energy due to absorption or scattering out of the path of the radiant flux, and the second and third terms are gains due to path radiance being scattered into the path of the radiant energy (either diffuse or collimated).

In many remote sensing applications, it may be justifiable to simplify the RTE to compare theory with observations. The purpose of this paper is to describe a set of analytical solution techniques, based on the simplification of the RTE, that utilizes the equations of irradiance (the two-flow equations) to quantitatively describe and predict the underwater light field. The analytical model takes two forms. In the Case I model, all irradiance is assumed to be

converted to diffuse irradiance immediately after it enters the water. In the Case II model, this assumption is not made. In other words, terms and equations are added to describe the influence of a specular or collimated irradiance component (i.e. direct sunlight) which is converted to the upwelling or downwelling diffuse or indirect light field. Derivations of the two flow equations used in these models from the RTE can be found in Mobley[5] (Case I), Ackleson[7] (Case II), Suits[8], Schuster[9], and Kubelka and Munk[10]. The analytical solution techniques used in both of the models have also been previously described[1,2,3]. The general solutions to the two-flow equations used here are similar to those given by the other authors, however, it is the boundary conditions described in the next section that make the specific forms of the equations used here unique.

In section two, we re-introduce the model equations. Section three of this paper deals with the choice of the conversion coefficient from direct, collimated irradiance to diffuse irradiance that is used in the Case II model. Section four describes new boundary conditions that can be used to allow both the Case I and Case II models to be layered (i.e., to apply the model to stratified water bodies where the intrinsic optical properties vary with depth). Section five describes and compares the output from the various versions of the model and output from a sensitivity analysis performed on the Case II model, and section six describes the applications and limitations of the model as well as indicating directions for further study. It should be noted that the analytical remote sensing model is also being applied to remote sensing of plant canopies[11].

2. MODEL EQUATIONS

2.1 Case I model[1,2,3]

The Case I model utilizes two first order, coupled differential equations to describe the upwelling and downwelling irradiances:

$$\frac{dE_d^w(z)}{dz} = -(a+b)E_d^w(z) + bE_u^w(z), \tag{2}$$

$$\frac{dE_u^w(z)}{dz} = (a+b)E_u^w(z) - bE_d^w(z), \tag{3}$$

where a is the absorption coefficient (m^{-1}) and b is the backscattering coefficient (m^{-1}), E_u is the upwelling irradiance (Wm^{-2}) and E_d is the downwelling irradiance (Wm^{-2}). Terms a and b are assumed constant in this case.

These equations can be solved with knowledge of the following unique, Cauchy type boundary conditions:

(1) $E_d(0)$, the downwelling irradiance at the surface z=0,

(2) $\frac{dE_d^w(0)}{dz}$, the downwelling slope, $\beta_d(0)$, at the surface z=0,

(3) $E_u(h)$, the upwelling irradiance at the bottom z=h where $E_u(h)=R_b*E_d(h)$, and R_b is the bottom reflectance,

(4) $\frac{dE_u^w(h)}{dz}$, the upwelling slope, $\beta_u(h)$, at the bottom z=h.

Equations 2 and 3 can be decoupled into two second order, linear, homogenous differential equations (the term homogeneous referring to the mathematical homogeneity of the equations, i.e., the equations are of the form y''+y'+y=0). The solutions to equations 2 and 3 are[1,3]:

$$E_d^w(z) = \frac{E_d^w(0)}{2}X + \frac{\beta_d(0)}{2\psi}Y, \tag{4}$$

$$E_u^w(z) = \frac{E_u^w(h)}{2} V - \frac{\beta_u(h)}{2\psi} W, \tag{5}$$

where

$$X = e^{\psi h} + e^{-\psi h}, \tag{6}$$

$$Y = e^{\psi h} - e^{-\psi h}, \tag{7}$$

$$V = e^{\psi(z-h)} + e^{-\psi(z-h)}, \tag{8}$$

$$W = e^{\psi(z-h)} - e^{-\psi(z-h)}, \tag{9}$$

h is the water column depth in meters, and z is the depth at which the irradiance is calculated.

2.1 Case II model[2]

The Case II model also utilizes a set of similar coupled, first order, non-homogeneous, differential equations. The additional terms and equation are introduced to explicitly describe the transfer of direct, collimated irradiance along with the indirect diffuse irradiance. The three equations for the Case II model are given below:

$$\frac{dE_d^w(z)}{dz} = -(a+b)E_d^w(z) + bE_u^w(z) + cE_s^w(z), \tag{10}$$

$$\frac{dE_u^w(z)}{dz} = (a+b)E_u^w(z) - bE_d^w(z) - cE_s^w(z), \tag{11}$$

$$\frac{dE_s^w(z)}{dz} = -\alpha E_s^w(z). \tag{12}$$

All terms are as defined in the Case I model, with the addition of c the conversion coefficient from specular, collimated irradiance to diffuse irradiance (m^{-1}), beam attenuation coefficient α (absorption plus total scattering) (m^{-1}), and E_s the specular or collimated irradiance.

Equations 10, 11 and 12 can be decoupled into two second order, linear, non-homogeneous differential equations (i.e., equations of the form y''+y'+y≠0). The solutions for downwelling, upwelling, and specular irradiances for the Case II model are given below in a slightly modified form from Bostater[2]:

$$E_d^w(z) = \frac{m + E_d^w(0)}{2} X + \frac{km - \beta_d(0)}{2\psi} Y - me^{kz}, \tag{13}$$

$$E_u^w(z) = \frac{ne^{kh} + E_u^w(0)}{2} V + \frac{kne^{kh} + \beta_u(h)}{2\psi} W - ne^{kz}, \tag{14}$$

$$E_s^w(z) = E_s^w(0)c^{\alpha z}, \tag{15}$$

where

$$n = \frac{c(k+a+2b)}{\left(k^2-\psi^2\right)} E_s(0), \tag{16}$$

$$m = \frac{-c(k-a-2b)}{\left(k^2-\psi^2\right)} E_s(0), \tag{17}$$

$$\psi = \sqrt{a^2+2ab}, \tag{18}$$

and V, W, X, and Y are as defined above for the Case I model.

The Case I and Case II model equations have similar solutions, however, one can easily note that additional terms are introduced into the Case II solutions due to the addition of the specular irradiance. *In both cases, the slope terms β_d and β_u are taken to be of the same form as the original differential equations*[1,2,3] (equations 2 and 3 for the Case I model and equations 10 and 11 for the Case II model).

3. THE CONVERSION COEFFICIENT

In the Case II model, a conversion coefficient from direct, specular irradiance to diffuse irradiance is used[8]. It is assumed in the Case II model that there is only a downwelling specular irradiance component, therefore only one conversion coefficient is used, and most of the direct light is converted to the indirect light or diffuse component before reaching the bottom. If specular irradiance does impinge upon the bottom, the bottom is considered to be a Lambertian surface, and all of the specular irradiance is converted to diffuse. Using Petzold's[12] volume scattering function (β) for turbid San Diego Harbor water, a backscattering coefficient can be found[7] by integrating β from $\pi/2$ to π. The result is a direct, or specular backscattering coefficient which can be multiplied by $1/\bar{\mu}$ (where $\bar{\mu}$ is the mean cosine of the light field) to find a diffuse backscattering coefficient. It was empirically determined, for the waters from the Banana River used in this study, that c=b*2.85 where b is the backscattering coefficient. It is assumed for this study that the conversion coefficient is the same in both directions, and thus the c's in equations 10 and 11 are the same. With reference to the sensitivity analysis results given later in this paper, it is obvious that more research is needed to properly parameterize this scattering effect or conversion coefficient as this is the most sensitive parameter in the model when collimated light (E_s) is a dominant term (Table 1).

Another parameter needed in the Case II model is α, the beam attenuation coefficient. The beam attenuation coefficient can be defined as the sum of absorption and total scattering, meaning that a relationship between the backscatter coefficient and the total scattering coefficient is needed. The total scattering coefficient for specular irradiance is taken to be on the order of 53 times the backscattering coefficient[13].

4. THE LAYERED MODEL

In order to layer the model, the use of the original differential equations for the slope terms described in section 2 (boundary conditions) needs to be reconsidered. This is due to the fact that, to compute β_d, we need *a-priori* knowledge of the upwelling irradiance at the bottom of the layer (the $E_u^w(z)$ term in equation 2 or equation 10). Since the solution procedure in the layered version of the two-flow model is to compute the downwelling irradiance at each layer interface down to the bottom and then to compute the upwelling irradiances back up to the surface, E_u is not known at each layer when computing E_d. Therefore, an alternate expression for the downwelling slope term can be used by describing it as a first-order differential equation as in Case I, but different, or:

$$\beta_d = \frac{dE_d}{dz} = -k_s' E_d. \tag{19}$$

The upwelling slope term, β_u, remains the same. Here k_s' is a type of attenuation coefficient for downwelling irradiance. A relation for k_s' at the water surface was developed from a quasi-single scattering formulation by Gordon[14]:

$$k_s' = \frac{a+b}{\mu}, \tag{20}$$

where μ is the cosine of the zenith angle of the incident light, a is absorption, and b is backscattering at or near the surface.

With reference to figure 1, using equation 4 or 13 for $E_d(1)$, equation 19 for β_d, and equation 20 for k_s', $E_d(1)$ and $E_d(0.5)$ (the midpoint between the first and second layers) can be calculated. Since Gordon's k_s' is only known to be valid at the surface, equation 19 is rearranged to find a new expression for k_s' at the surface in order to calculate E_d at the bottom of the second layer:

$$k_s' = -\frac{1}{E_d(0.5)} \frac{dE_d(z)}{dz}, \tag{21}$$

where the derivative in equation 21 is calculated over the bottom half of the first layer as:

$$\frac{dE_d(z)}{dz} = \frac{E_d(1) - E_d(0.5)}{z(1) - z(0.5)}. \tag{22}$$

For all layers after the second, the derivative in 21 is calculated between the midpoints of the layers as:

$$\frac{dE_d(z)}{dz} = \frac{E_d(i) - E_d(i-0.5)}{z(i) - z(i-0.5)}, \tag{23}$$

where i is the current layer and can range from i=1 to N layers. This technique represents a calculation procedure where the layer and calculation domains are staggered.

In the case of upwelling irradiances, β_u is assumed to have the form of the original differential equation, or:

$$\beta_u = \frac{dE_u(i)}{dz} = (a_{i+1} + b_{i+1}) E_u(i+1) - b_{i+1} E_d(i+1), \tag{24}$$

where i is the layer to calculate E_u for. In this case, the absorption and backscatter coefficients (a and b) *from the previous layer* are assumed to act as in a thin water bottom boundary layer. Physically, this allows one to consider different absorption and backscatter coefficients unique to different bottom types or water near the bottom. This formulation also allows different absorption and backscatter coefficients near the surface which may include different effects such as surface waves (e.g. capillary, gravity waves, and wave focusing effects).

5. APPLICATION AND TESTING OF THE MODEL

The Banana River is a shallow, turbid lagoon on the east-central coast of Florida (Figure 6). On January 30, 1996, measurements of the absorption coefficient in the Banana River were made using a long path length absorption cuvette[16,17]. These measurements were used to calculate backscatter coefficients according to the formula $b=R_a(0)*a/0.23$[15] where $R_a(0)$ is the reflectance just above the water surface. The conversion coefficient was calculated as described in Section 3. The

bottom reflectance was taken to be 0.001 at each wavelength. These parameters were used as input into both cases of the model, and the model derived above water reflectance signatures were compared with measured reflectance signatures taken at the same time as the water samples were taken. The layered version of the Case I model was also run using the above parameters, and the output from all three models is shown in Figure 2 along with the measured reflectance signature.

In addition, a sensitivity analysis was performed on the Case II model. The sensitivity analysis was performed at three separate wavelengths: 430, 490, 540. These wavelengths were chosen since the dissolved organic carbon absorption maximum occurs near 430 nm[16,17], the maximum penetration of solar energy occurs at 490 nm, and the hinge point of chlorophyll (where the reflectance is independent of chlorophyll concentration) occurs around 540 nm. A sensitivity parameter was calculated using the method described by Bostater[18]. Earlier research reported in Bostater, et al.[2] indicated that a and b were the most sensitive parameters in the Case I model. The results of our new sensitivity analysis for the Case II model indicates that the conversion coefficient is the most sensitive parameter, followed by the beam attenuation coefficient, absorption coefficient, and backscatter coefficient. Results of the sensitivity analysis are tabulated in Table 1.

Figure 2 is a comparison of the output from the various models with measured reflectance signatures. The same absorption, backscatter, and bottom reflectance spectra were used as input into each model. Figure 3 shows graphical output from the layered Case I model with 10 layers. The layered model allows for a more detailed vertical distribution of the intrinsic optical properties (i.e., those properties whose value is indpendent of the distribution of the light field) in a water body. Figure 3 shows output from the layered model using the absorption and backscatter coefficients for pure sea water in each layer. Output is also shown for pure sea water with 20 μg/L chlorophyll in the upper two meters (surface layer 1 of 10) of a 20 meter water column to roughly simulate a surface algal bloom, and for pure sea water with 20 g/L of suspended sediments in the bottom two meters (bottom layer 10 of 10) of a 20 meter water column simulating resuspension of bottom sediments. Figures 4-7 show the penetration of light at four selected wavelengths under the influence of different water quality concentrations from the layered Case I model.

6. CONCLUSIONS AND DIRECTIONS FOR FURTHER STUDY

The two-flow irradiance model described and applied in this paper is capable of generating realistic reflectance signatures when given input as to the absorption and backscatter coefficients (Case I and II), and conversion and beam attenuation coefficients (Case II). Results of the sensitivity analysis indicate, as expected, that the model is most sensitive to these parameters. From a modeling standpoint, the route chosen to obtain these coefficients is of primary importance as they are the parameters that drive the system that generates the reflectance signatures.

The analytical two-flow models described here have been shown to be capable of reproducing realistic reflectance signatures given the proper coefficients as input. The Case I model underestimates the measured reflectance, while the Case II model, in general, overestimates the reflectance when the same parameters are used. Both cases of the model have useful applications to aquatic[19] as well as terrestrial[11] systems. Results of the sensitivity analyses indicate that, for the Case II model, the most sensitive coefficients are the conversion, attenuation, absorption, and backscatter coefficients. For the Case I model, the most sensitive input parameters are absorption, backscatter, and bottom reflectance[2]. More research needs to be conducted to determine if the added complexity of the Case II model (addition of the specular irradiance) is justified, or if the Case I model is adequate. Specifically, methods need to be developed to accurately quantify bottom types and better estimate the various coefficients in the model[16,17].

7. ACKNOWLEGEMENTS

8. REFERENCES

1. C. Bostater, W. Ma, and A. Lamb, "Simulating radiative transfer in aquatic systems and contrasting results from ambient environmental spectroscopy: estuarine and near coastal waters," In: *Proc. 2nd Intl. Symp. on Spectral Sensing Research*, San Diego, CA, USACOE, July, 1994, pp. 673-682.

2. C. Bostater, W. Ma, T. McNally, M. Gimond, and A. Lamb, "Application of an optical remote sensing model," In: *Proc. European Optical Society and SPIE - The International Society for Optical Engineering (EUROPTO), The European Symposium on Satellite Remote Sensing*, Paris, France, 25-28 September, 1995, Volume 2586, pp. 32-43.

3. A. Lamb, Sensitivity analysis of an optical remote sensing model, Master Thesis, Florida Institute of Technology, 1995, 136 pp.

4. N. Jerlov, *Marine Optics*, Elsevier Oceanography Series, 14, 1976, 231 pp.

5. C. Mobley, *Light and Water: Radiative Transfer in Natural Waters*, Academic Press, San Diego, CA, 1994, 592 pp.

6. R. Priesendorfer, *Hydrologic Optics*, Vol I-VI, NOAA/ERL, Honolulu, HI, 1976, 1757 pp.

7. S. Ackleson, A two-flow model to simulate the interaction of irradiance with a submerged plant canopy, Ph.D. Dissertation, University of Delaware, 1985, 139 pp.

8. G. Suits, "The Calculation of the Directional Reflectance of a Vegetative Canopy," *Remote Sens. Env.*, 1972, 2, 117.

9. A. Schuster, "Radiation through a foggy atmosphere," *Astrophys. J.*, 21(1), 1905, 1-22.

10. P. Kubelka, and F. Munk, "Ein Beitrag zur optik der Farbanstriche," *Z. Tech. Physik* 12, 593, 1931.

11. M. Pegaz, C. Bostater, and C. Hall, "Application of an analytical two-flow radiative transfer model to plant canopies," in press, Proc: *Eco-Informa '96*, Lake Buena Vista, FL, 4-7 November, 1996.

12. T. Petzold, Volume scattering functions for selected ocean waters, SIO Ref. 72-78, Scripss Inst. Oceanogr., La Jolla, 79 pp. Condensed as Chapter 12 in Light in the Sea, Edited by J.E. Tyler, Dowden, Hutchinson & Ross, Stroudsberg, 1977, 150-174.

13. J. Kirk, *Light and Photosynthesis in Aquatic Ecosystems*, 2nd Ed., Cambridge University Press, Cambridge, UK, 1994, 509 pp.

14. H. Gordon, Modeling and Simulating Radiative Transfer in the Ocean, In: *Ocean Optics*, ed. R. W. Spinrad, K. L. Carder, and M. J. Perry, Oxford University Press, New York, NY, 1994, 283 pp.

15. C. Bostater, W. Ma, T. McNally, M. Gimond, M. Keller, and M. Pegaz, "Comparison of an optical remote sensing reflectance model with reflectance signatures collected from an airborne sensor platform," In: *Proc. 2nd Intl. Airborne Remote Sensing Conference and Exhibition*, San Francisco, CA, 24-27 June, 1996, Volume 3, pp. 647-656.

16. C. Bostater and M. Gimond, "Methodology evaluation for remotely estimating water quality parameters in estuarine waters," In: *Proc. European Optical Society and SPIE - The International Society for Optical Engineering (EUROPTO), The European Symposium on Satellite Remote Sensing,* Paris, France, 25-28 September, 1995, Volume 2586, pp. 14-25.

17. C. Bostater and M. Gimond, "Using aircraft based high resolution reflectance signatures and specific absorption coefficients to remotely estimate coastal water quality," In: *Proc. 2nd Intl. Airborne Remote Sensing Conference and Exhibition*, San Francisco, CA, 24-27 June, 1996, pp. 635-645.

18. C Bostater, On simulating the active vertical motion of *Morone saxatilis* in the estuarine environment, Ph.D. Dissertation, University of Delaware, 1989, 207 pp.

19. C. Bostater, T. McNally, and W. Ma, "Modeling of the underwater light field and its effect on circulation," in press: *Proc. European Optical Society and SPIE - The International Society for Optical Engineering (EUROPTO), The European Symposium on Satellite Remote Sensing*, Taormina, Italy, 23-27 September, 1996.

20.

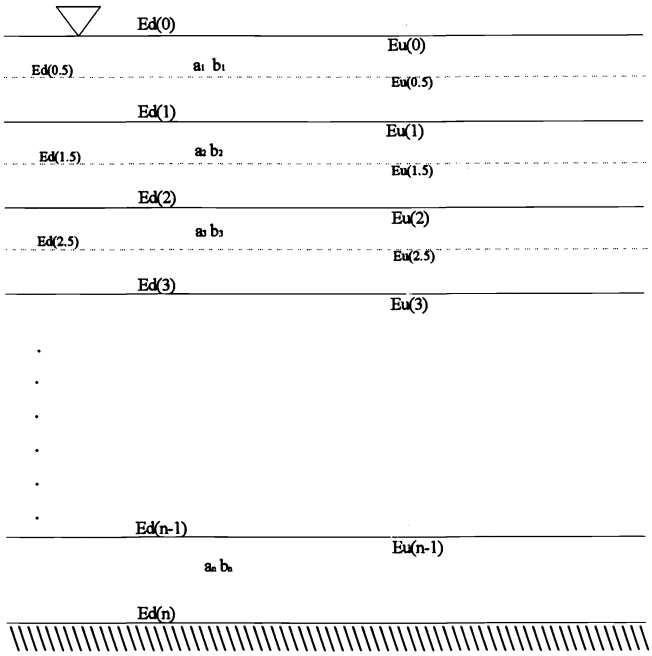

Figure 1. Schematic showing the computational domain of the layered model. Full lines denote boundaries between layers, and dashed lines are midpoints of the layers. The absorption and backscatter coefficients are assumed constant within each layer, but may be different from layer to layer.

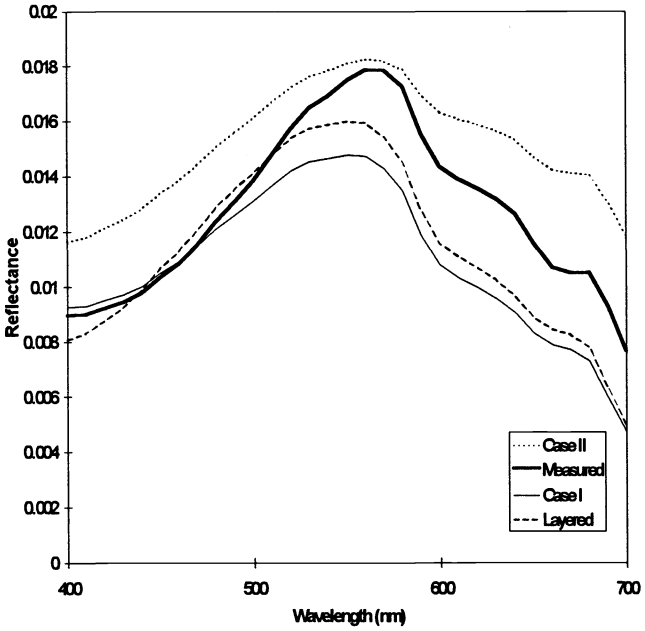

Figure 2. Comparison of model derived above water reflectance spectra from the three models with the reflectance measured in the Banana River. Bottom reflectance is 0.001.

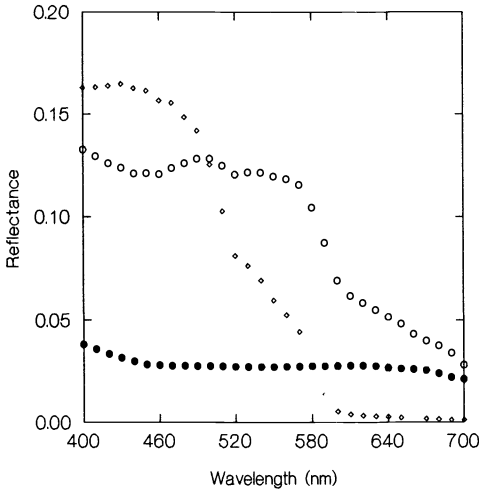

Figure 3. Model derived subsurface reflectance spectra generated by the layered Case I model (10 layers). In descending order, the spectra are for: pure sea water (squares), 20 mgL^{-1} seston in the bottom 2 meters (circles), and 20 μgL^{-1} chlorophyll in the top 2 meters (full circles). h=20m. Bottom reflectance is 0.05 across the spectrum.

Model Variable	Normalized Sensitivity 430 nm	490 nm	540 nm
Absorption coefficient	0.82 (2.39)	0.64 (2.06)	0.49 (1.99)
Backscatter coefficient	0.48 (2.64)	0.37 (2.24)	0.31 (2.09)
Bottom Reflectance	0.02 (2.72)	0.00 (2.27)	0.01 (2.12)
Specular irradiance	0.16 (2.73)	0.14 (2.29)	0.12 (2.13)
Downwelling irradiance	0.16 (2.67)	0.12 (2.24)	0.11 (2.09)
Refractive index of air	0.00 (0.00)	0.00 (0.00)	0.00 (0.00)
Refractive index of water	0.00 (0.00)	0.00 (0.00)	0.00 (0.00)
Water depth	0.59 (2.64)	0.60 (2.19)	0.64 (2.01)
Conversion coefficient	1.00 (2.49)	1.00 (2.02)	1.00 (1.84)
Beam attenuation coefficient	0.79 (2.24)	0.79 (1.81)	0.78 (1.68)

Table 1. Tabulated results of the sensitivity analysis on the Case II model. Note that the conversion coefficient is always the most sensitive parameter followed by either the absorption or beam attenuation coefficient. Values in parentheses are the standard deviations for the sensitivity of each parameter.

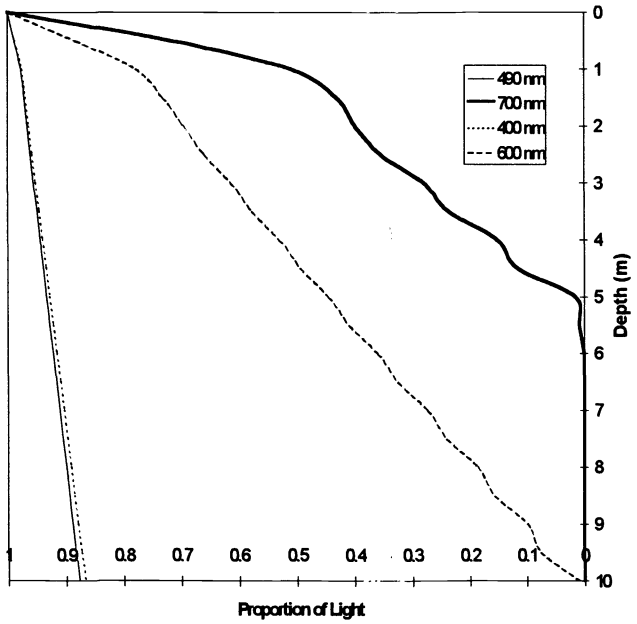

Figure 4. Output from the layered Case I model showing penetration of light at four selected wavelengths. Bottom reflectance is 0.05 across the spectrum, and h=10m (10 layers). This run was made using pure sea water only.

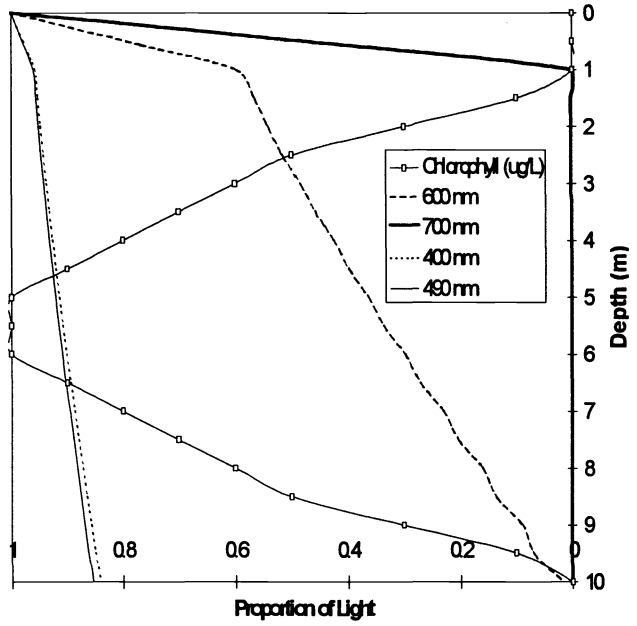

Figure 5. Output from the layered Case I model showing penetration of light at four selected wavelengths. Bottom reflectance is 0.05 across the spectrum, and h=10 (10 layers). The vertical distribution of chlorophyll (normalized to 20 μgL^{-1}) is also shown.

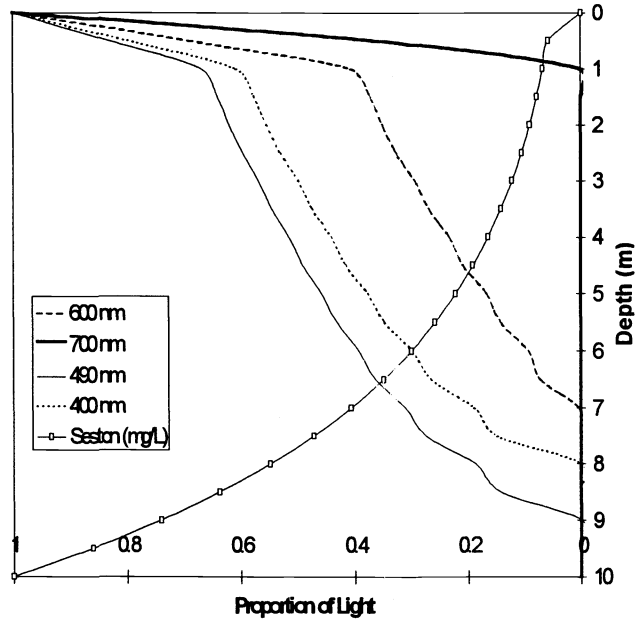

Figure 6. Output from the layered Case I model showing penetration of light at four selected wavelengths. Bottom reflectance is 0.05 across the spectrum, and h=10 m (10 layers). The vertical distribution of seston (normalized to 20 mgL^{-1}) is also shown.

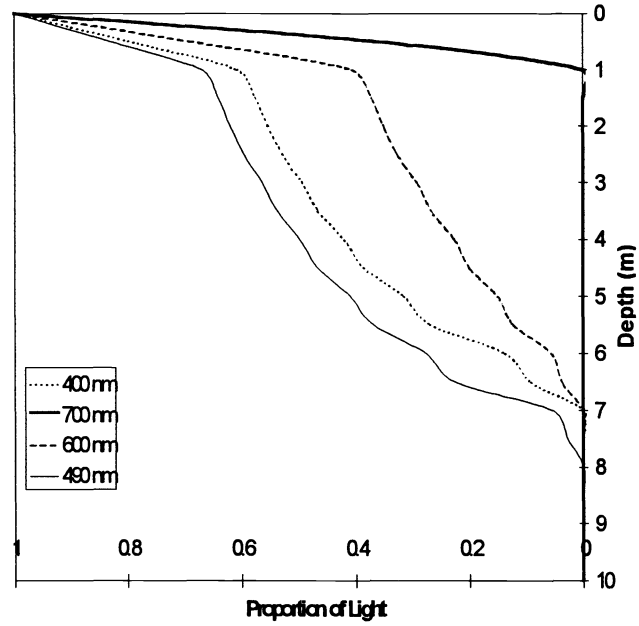

Figure 7. Output from the layered Case I model showing penetration of light at four selected wavelengths. Bottom reflectance is 0.05 across the spectrum, and h=10m (10 layers). This run used the vertical distribution of seston *and* chlorophyll from Figures 4 and 5.